Visualisation and classification of dynamic structural health monitoring data for assessment of structural condition

O.R de Lautour & P. Omenzetter

Department of Civil and Environmental Engineering, University of Auckland, Auckland, New Zealand.

2008 NZSEE Conference

ABSTRACT: With the advent of modern sensing technology, monitoring of structures under dynamic excitation becomes a viable option for quick assessment of their condition and health. However, major challenges still exist in interpreting the monitoring data. The application of time series analysis methods to Structural Health Monitoring (SHM) is a relatively new but promising approach. Time series methods are inherently suited to SHM where data is sampled regularly over a long period of time, which is typical for monitoring systems. This study focuses on the classification of damage based on analysis of time series model coefficients. Autoregressive (AR) models were used to fit the acceleration time histories of a 3-storey laboratory bookshelf structure and data collected from the ASCE Phase II SHM Benchmark Structure in both healthy and damaged states. Preliminary inspection of the multivariate AR coefficients to check the presence of clusters corresponding to different damage states was achieved using two-dimensional projections obtained from either Principal Component Analysis (PCA) or Sammon mapping. Two classification techniques, Nearest Neighbour Classification (NNC) and Learning Vector Quantisation (LVQ) were used to classify damage into states based on analysis of the AR coefficients reduced in dimensionality via PCA. The results showed that NNC performed well, however, small improvements could be made using LVQ.

1 INTRODUCTION

For New Zealand, a country with well-developed and extensive built infrastructure, located in an area of high seismicity, the prospect of being able to quickly assess the condition and health of structures following seismic or other potentially dangerous events using data collected by sensor arrays, such as Geonet, is very useful. Methods that try to achieve this are referred to as Structural Health Monitoring (SHM). Over the two past decades considerable research efforts have focused on developing robust and reliable approaches to SHM (Doebling et al. 1996, Sohn et al. 2003), amongst which vibration based techniques are the most widely used and appear to be the most promising. However, considerable challenges still exist in making sense of the large volumes of monitoring data so that they can be used in a meaningful way and provide information on structural condition that would be useful for infrastructure owners, users, and emergency planning and response authorities.

This research focuses on the application of times series analysis for detection and classification of damage in civil infrastructure. Time series analysis techniques, originally developed for analysing long sequences of regularly sampled data are inherently suited to SHM. However, applications of such techniques for SHM can still be considered as an emerging technique and remain relatively unexplored. An interesting and promising approach is to use time series model coefficients as damage sensitive features. A pioneering study by Sohn et al. (2000) used Autoregressive (AR) models to fit the dynamic response of a concrete bridge pier. By performing statistical analysis on the coefficients of the AR models the authors were able to distinguish between the healthy and damaged structure. In a later study, Sohn et al. (2001) applied a similar methodology to health monitoring of a surface-effect fast patrol boat. However, these studies focused only on damage detection and the authors did not attempt to assess its severity. Gul et al. (2007) presented a study in which AR coefficients from a laboratory steel beam with varying support conditions were classified using a clustering algorithm.

Omenzetter and Brownjohn (2006) used a vector Seasonal Autoregressive Integrated Moving Average model to detect abrupt changes in strain data collected from the continuous monitoring of a major bridge structure. The seasonal model was used because of the strong diurnal component in the data caused by temperature variations. Nair et al. (2006) used an Autoregressive Moving Average time series to model vibration signals from the ASCE Phase II Experimental Benchmark Structure. The authors defined a damage sensitive feature used to discriminate between the damaged and undamaged states of the structure based on the first three AR coefficients. The localisation of the damage was achieved by introducing another feature, also based on the AR coefficients, found to increase from a baseline value when damage was near. In a later study, Nair and Kiremidjian (2007) used Gaussian Mixtures Modelling to analyse clusters of AR coefficients corresponding to the different damage states from the same structure.

This study addresses the problem of making sense of the SHM measurements by studying analytical methods for visualisation and automatic classification of data corresponding to different structural damage states. AR models were used to fit the dynamic response of a simple 3-storey laboratory structure and data collected from the more complex ASCE Phase II Experimental Benchmark Structure in both damaged and undamaged states. The coefficients of those models were used as the damage sensitive feature. One of the challenges was to reduce the dimensionality of the feature so that it could be easily inspected. To that end, clustering in the AR coefficients was investigated via two-dimensional projections using the techniques of Principal Component Analysis (PCA) and Sammon mapping. Another addressed challenge was to classify automatically features corresponding to different damage states. Two analytical techniques, Nearest Neighbour Classification (NNC) and Learning Vector Quantisation (LVQ) were applied to the AR coefficients reduced in dimensionality using PCA.

2 THEORY

2.1 *Autoregressive models*

In this study, AR time series models are used to describe the acceleration time histories. AR models are used in the analysis of stationary time series processes and attempt to account for the correlations of the current observation in a time series with its predecessors. A univariate AR model of order p, or AR(p), for the time series $\{x_t\}$ (t = 1,2,…n) can be written as

$$x_t = \phi_1 x_{t-1} + \phi_2 x_{t-2} + ... + \phi_p x_{t-p} + a_t \tag{1}$$

where x_t,…x_{t-p} are the current and previous values of the analysed series $\{x_t\}$ and $\{a_t\}$ is a Gaussian white noise error time series with a zero mean and constant variance. The AR coefficients ϕ_1,…, ϕ_p can be evaluated using a variety of methods (Wei 2006). A least-squares solution was adopted in this study.

2.2 *Nearest Neighbour Classification*

Nearest Neighbour Classification is a simple supervised pattern recognition technique (Kohonen 1997). Given a set of pre-selected and fixed reference or codebook vectors $\mathbf{m}_i$ (i = 1, …, k) corresponding to known classes, an unknown input vector $\mathbf{x}$ is assigned to the class to which the nearest $\mathbf{m}_i$ belongs. Several distance measures can be used including Manhattan, Euclidean, Correlation and Mahalanobis. In this study, the Euclidean and Mahalanobis distance measures were used. The Euclidean distance $D_E(\mathbf{x},\mathbf{y})$ between two vectors $\mathbf{x}$ and $\mathbf{y}$ can be calculated using

$$D_E(\mathbf{x},\mathbf{y}) = \sqrt{(\mathbf{x}-\mathbf{y})^T(\mathbf{x}-\mathbf{y})} \tag{2}$$

where superscript T denotes transposition. The Mahalanobis distance $D_M(\mathbf{x},\mathbf{y})$ between two vectors of the same multivariate distribution with a covariance matrix $\mathbf{\Sigma}$ can be calculated from

$$D_M(\mathbf{x},\mathbf{y}) = \sqrt{(\mathbf{x}-\mathbf{y})^T \mathbf{\Sigma}^{-1} (\mathbf{x}-\mathbf{y})} \tag{3}$$

The Mahalanobis distance accounts explicitly for the different scales and correlations amongst vector entries and can be more useful in cases where these are significant.

2.3 *Learning Vector Quantisation*

Learning Vector Quantisation is a technique designed for classification by defining class borders (Kohonen 1997). It is similar to NNC in that it uses a set of codebook vectors and seeks the minimum distance of an unknown vector to these codebook vectors as the criterion for classification. However, unlike NNC where codebook vectors are fixed, an iterative procedure is adopted in which the position of the codebook vectors is adjusted to minimise the number of misclassifications. Learning of the optimal codebook vector positions can be performed using several algorithms. In this study, the Optimised-Learning-Rate LVQ1 algorithm was used. This algorithm has an individual learning rate for each codebook vector, resulting in faster training.

Given a set of initial codebook vectors $\mathbf{m}_i$ (i = 1, …, k) which have been linked to each class region, the new input vector $\mathbf{x}$ is assigned to the class which the nearest $\mathbf{m}_i$ belongs, i.e. an NNC task is performed. Let c define the index of the nearest codebook vector, i.e. $\mathbf{m}_c$. Learning is an iterative procedure in which the position of the codebook vectors is adjusted to minimise the number of misclassifications. At iteration step t let $\mathbf{x}(t)$ and $\mathbf{m}_i(t)$ be the input vector and codebook vectors respectively. The $\mathbf{m}_i(t)$ are adjusted according to the following learning rule

$$\begin{aligned} \mathbf{m}_c(t+1) &= \left[1 - s(t)\alpha_c(t)\right]\mathbf{m}_c(t) + s(t)\alpha_c(t)\mathbf{x}(t) \\ \mathbf{m}_i(t+1) &= \mathbf{m}_i(t) \text{ for } i \neq c \end{aligned} \tag{4}$$

where $s(t)$ equals +1 or -1 if $\mathbf{x}(t)$ has been respectively classified correctly or incorrectly, and $\alpha_c(t)$ is the variable learning rate for codebook vector $\mathbf{m}_c$:

$$\alpha_c(t) = \frac{\alpha_c(t-1)}{1 + s(t)\alpha_c(t-1)} \tag{5}$$

The learning rate must be constrained such that $\alpha_c(t) < 1$.

2.4 *Principal Component Analysis*

Principal Component Analysis is a popular multivariate statistical technique often used to reduce multidimensional data sets to lower dimensions (Sharma 1997). Given a set of p-dimensional vectors $\mathbf{x}_i$ (i = 1, …, n) drawn from a statistical distribution with mean $\bar{\mathbf{x}}$ and covariance matrix $\mathbf{\Sigma}$, PCA seeks to project the data into a new p-dimensional space with orthogonal coordinates via a linear transformation. Decomposition of the covariance matrix by singular value decomposition leads to

$$\mathbf{\Sigma} = \mathbf{V}\mathbf{\Lambda}\mathbf{V}^T \tag{6}$$

where $\mathbf{\Lambda}$ = diag[σ_1^2, …, σ_p^2] is a diagonal matrix containing the eigenvalues of $\mathbf{\Sigma}$ ranked in the

descending order $\sigma_1^2 \geq \ldots \geq \sigma_p^2$, and $\mathbf{V}$ is a matrix containing the corresponding eigenvectors or principal components. The transformation of a data point $\mathbf{x}_i$ into principal components is

$$\mathbf{z}_i = \mathbf{V}^T \left(\mathbf{x}_i - \bar{\mathbf{x}} \right) \tag{7}$$

The new coordinates $\mathbf{z}_i$ are uncorrelated and have a diagonal covariance matrix $\mathbf{\Lambda}$. Therefore, the entries of $\mathbf{z}_i$ are linear combinations of the entries of $\mathbf{x}_i$ which explain variances $\sigma_1^2, \ldots, \sigma_p^2$. To reduce the dimensionality, a selection $q < p$ of principal components can be used that retains those components that contribute most to the data variance, thus reducing the dimension of the data to q.

2.5 *Sammon Mapping*

Sammon mapping (Sammon 1969) is a nonlinear transformation used for mapping a high dimensional space to a lower dimensional one in which local geometric relations are approximated. Consider a set of vectors $\mathbf{x}_i$ (n = 1, …, n) in a p-dimensional space and a corresponding set of vectors $\mathbf{y}_i$ in a q-dimensional space, where $q < p$. For visualisation purposes q is usually chosen to be two or three. The Euclidean distance between vectors $\mathbf{x}_i$ and $\mathbf{x}_j$ in p-dimensional space is D_{ij}^* and the distance between the corresponding vectors $\mathbf{y}_i$ and $\mathbf{y}_j$ in q- dimensional space is D_{ij}. Mapping is achieved by adjusting the vectors $\mathbf{y}_i$ to minimise the following error function by steepest descent

$$E = \frac{1}{\sum_{i=1}^{n} \sum_{j<i} D_{ij}^*} \sum_{i=1}^{n} \sum_{j<i} \frac{\left(D_{ij} - D_{ij}^* \right)^2}{D_{ij}^*} \tag{10}$$

3 APPLICATION TO A 3-STOREY BOOKSHELF STRUCTURE

The 3-storey experimental bookshelf structure used in this study was approximately 2.1m high and constructed from equal angle aluminium column sections and stainless steel floor plates bolted together with aluminium brackets as shown in Figure 1. The stainless steel plates were 4mm thick and 650mm × 650mm square. The column sections were 30mm × 30mm equal angles. Two section thicknesses were used for the columns, either 3.0mm or 4.5mm for the damaged and undamaged states respectively. Each column was made of 3 × 0.7m high segments, rather than one long angle, in order to make them easily replaceable for simulation of localized damage at different stories. The column sections were fastened at each end with two M6 bolts to aluminium brackets (Figure 1b). Additional brackets were installed at the base of the structure to minimise torsional motion. The whole structure was mounted on a 20mm plywood sheet fixed with M10 bolts to the shake table.

The structure was instrumented with four uniaxial accelerometers, one for measuring the table acceleration and one for each storey. Accelerations were measured in the direction of ground motion at 400Hz using a computer fitted with a data-logging card. Afterwards the data was decimated by a factor of four for modal analysis and eight for time series modelling.

Damage was introduced into the structure by replacing the original 4.5mm thick columns of a particular storey with 3.0mm angles. Four damage states were considered; these were labelled D0, D1, D2 and D3 corresponding to no damage (healthy structure), 1st storey damage, 2nd storey damage and simultaneous 1st and 2nd story damage. From the results of modal analysis simple mass-spring models of the structure were updated. This allowed the reduction in stiffness caused by the changing columns to be estimated. Figure 2 schematically shows these four damage states together with the percentage of remaining stiffness obtained via model updating.

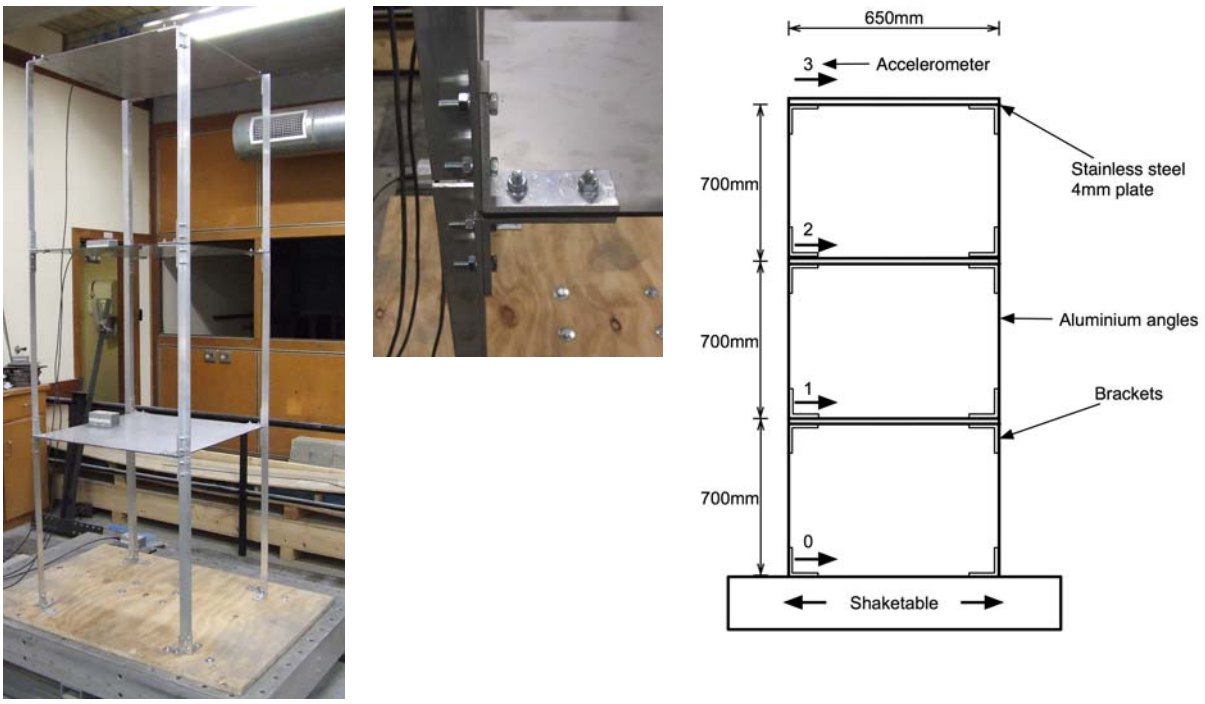

(a) (b) (c)

Figure 1. 3-storey bookshelf structure (a) general view, (b) detail of column-floor joint, and (c) dimensions and accelerometer locations.

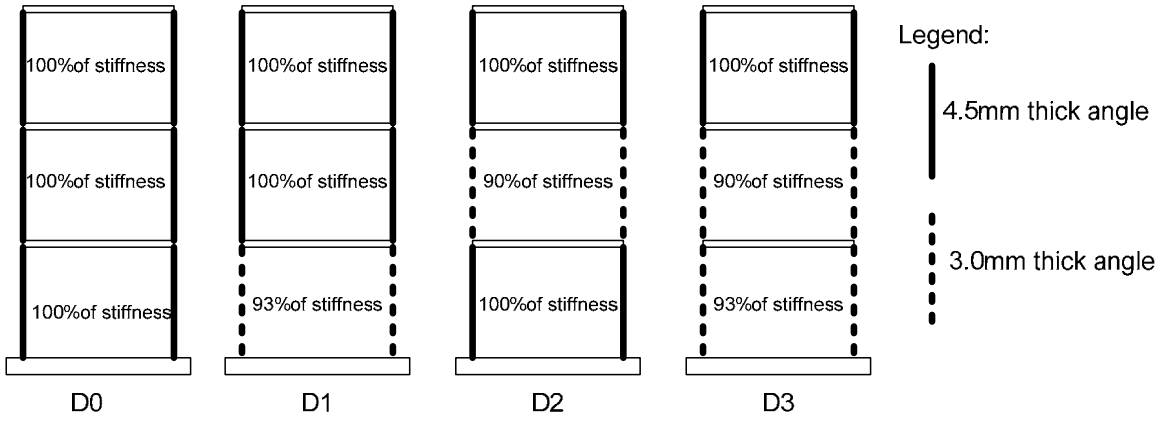

Figure 2. Damage states in 3-storey structure showing percentage of lateral stiffness at each floor.

The objective of the damage detection study was to classify seismic responses measured in the four damage states and to that end eight scaled earthquake records were used to excite the structure. Table 1 lists the earthquakes used, the Peak Ground Acceleration (PGA) of the original and scaled records, the duration of the record and the frequency at which the earthquake was sampled. The earthquakes were scaled so that a range of response amplitudes was obtained, while ensuring no yielding of the structure occurred.

The acceleration time history of each storey was modelled using a univariate AR model. AR(12) models were determined to give both a sufficient fit to the acceleration data and had no significant correlation in the residual errors. The AR coefficients were estimated from a 500-point window advancing 100 points until the end of the record was reached. A least squares approach was used to calculate the AR coefficients. A data set of 388 points (vectors of AR coefficients) containing 97 points for each damage state was obtained.

Table 1. Earthquake records used to excite 3-storey bookshelf structure.

Earthquake	PGA (g)	Scaled PGA (g)	Duration (sec)	Sampling frequency (Hz)
Duzce 12/11/1999	0.535	0.027	25.885	200
Erzincan 13/3/1992	0.496	0.033	20.780	200
Gazli 17/5/1976	0.718	0.048	16.265	200
Helena 31/10/1935	0.173	0.035	40.000	100
Imperial Valley 19/5/1940	0.313	0.031	40.000	100
Kobe 17/1/1995	0.345	0.035	40.960	100
Loma Prieta 18/10/1989	0.472	0.047	39.945	200
Northridge 17/1/1994	0.568	0.038	40.000	50

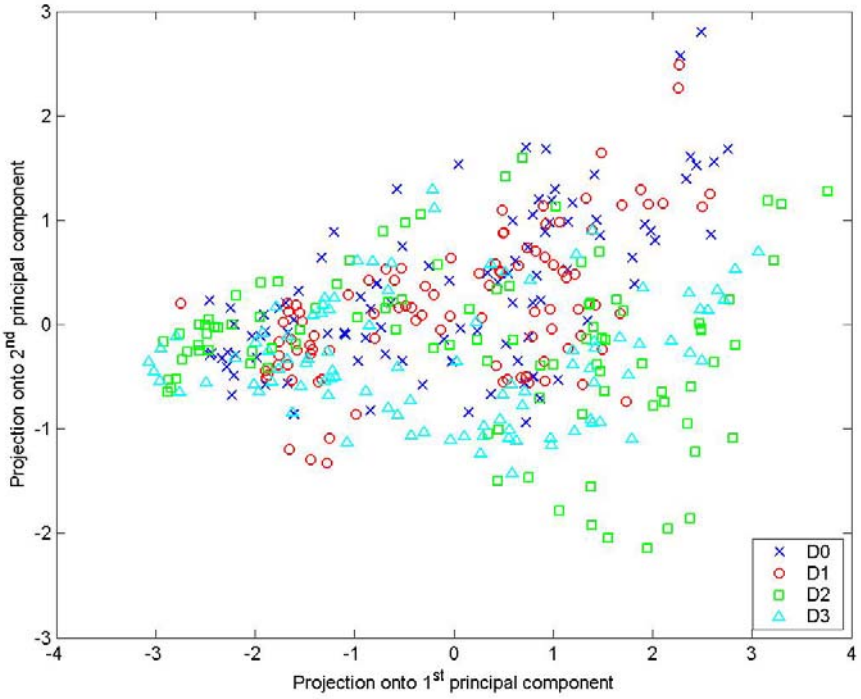

Figure 3. Projection of data from 3-storey bookshelf structure onto the first two principal components.

3.1 *Damage classification in the 3-storey bookshelf structure*

Using three univariate AR(12) models, one for each floor, resulted in 36-dimensional vectors of damage sensitive features. As a preliminary investigation, to visualise and check the presence of clusters in the data, PCA and Sammon mapping were used to create two and three-dimensional projections of the vectors of AR coefficients. The results of the two-dimensional projections are shown in Figures 2 and 3 for PCA and Sammon mapping, respectively. Projection of the data onto the first two principal components showed no clearly defined clusters with data points from all four damage states scattered amongst one another. In contrast, the Sammon map showed some organisation of the data into overlapping bands, although again, no distinct clusters could be drawn. Using three-dimensional mappings did not provide a better separation. These preliminary insights indicate that higher dimensional data need to be investigated to achieve separation of the AR coefficients from

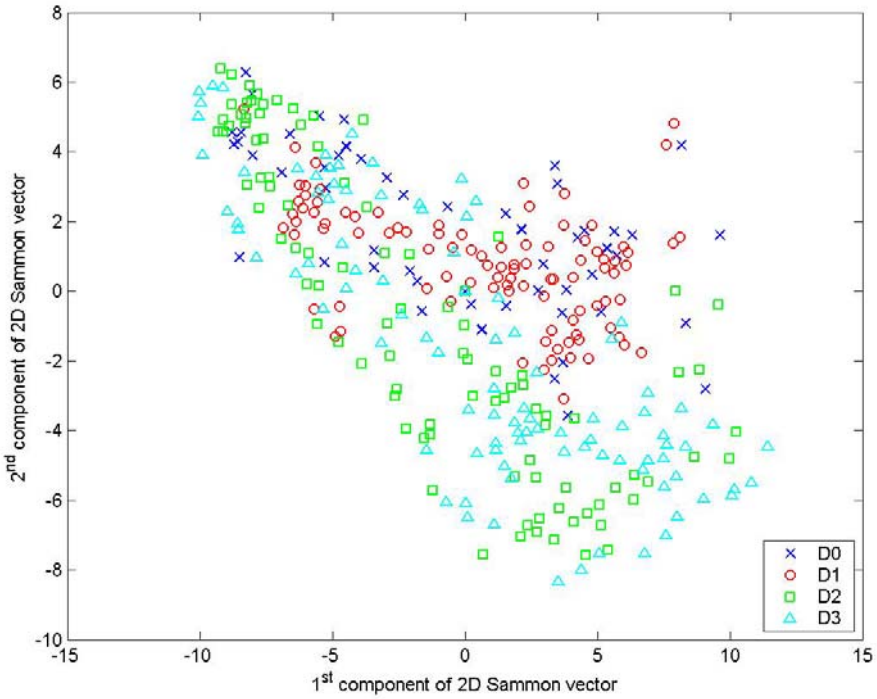

Figure 4. Projection of data from 3-storey bookshelf structure via Sammon mapping.

Table 2. Number and percentage of misclassification using NNC for 3-storey bookshelf structure.

Number of principal components	Euclidean distance	Mahalanobis distance
30	17 (19.3%)	1 (1.1%)
20	16 (18.2%)	1 (1.1%)
10	16 (18.2%)	6 (6.8%)
5	27 (30.7%)	24 (27.3%)

Table 3. Number and percentage of misclassifications using LVQ for 3-storey bookshelf structure.

Number of principal components	Number of codebook vectors		
	30	50	100
30	0 (0%)	0 (0%)	0 (0%)
20	0 (0%)	0 (0%)	0 (0%)
10	14 (15.9%)	10 (11.4%)	5 (5.7%)

different damage states. Simple visual techniques will then be inadequate and more advanced approaches such as NNC and LVQ need to be used.

The two previously described classification techniques, NNC and LVQ where used to classify damage into the states D0-D3. The feature dimension was reduced by projecting the data using PCA onto either the first 30, 20, 10 or 5 principal components. PCA only was chosen for dimensionality reduction because it is much faster than Sammon mapping. The set of 388 available vectors of AR coefficients was randomly divided into 300 codebook vectors and 88 testing points. A total of five

simulations were performed with different codebook vectors. The averaged numbers of misclassifications and percentage errors from five runs using NNC with either Euclidian or Mahalanobis distance measure are given in Table 2. The Mahalanobis distance measure outperformed the Euclidean by a considerable margin. Reasonably good results with 6.8% of misclassifications were obtained for the Mahalanobis distance measure using only 10 principal components. Increasing the number of principal components to 20 or 30 further reduced the numbers of misclassifications to 1.1%. On the other hand, NNC using the Euclidian distance measure still produced 19.3% of misclassifications even when 30 principal components were used. The significantly better performance of the Mahalanobis distance measure can be explained by the fact that it accounts for the different scales of each principal component.

Although NNC performed well, performance could be improved by using a more advanced and flexible classification technique such as LVQ. As the previous analysis demonstrated that the Mahalanobis measure achieved a superior performance, only this measure was used with LVQ classification. The 388-point data set was divided into 300 points for training and 88 points for testing. The number of codebook vectors was chosen to be 30, 50 or 100. These were initialised by random selection from the training data set. The averaged results from five runs with different initial selections of codebook vectors, given in Table 3, show that increasing the number of codebook vectors and

(a)  (b) 

Figure 5. ASCE Phase II Experimental SHM Benchmark Structure: (a) general view, and (b) beam-column joint.

Table 4. Damage configurations for ASCE Phase II Experimental SHM Benchmark Structure.

Configuration	Damage
1	No damage
2	All bracing removed on the E face
3	Bracing removed on floors 1-4 on a bay on the SE corner
4	Bracing removed on floors 1 and 4 on a bay on the SE corner
5	Bracing removed on floors 1 on a bay on the SE corner
6	All bracing removed on E face and floor 2 on N face
7	All bracing removed
8	Configuration 7 + loosened bolts on floors 1-4 on E face N bay
9	Configuration 7 + loosened bolts on floors 1 and 2 on E face N bay

principal components used reduced the number of misclassifications. For 20 or more principal components and 30 or more codebook vectors perfect classification results were achieved. Overall, an improvement over NNC was also observed.

4 APPLICATION TO ASCE PHASE II EXPERIMENTAL SHM BENCHMARK STRUCTURE

The ASCE Phase II Experimental SHM Benchmark Structure (ASCE 2002) is a 4-storey 2-bay by 2-bay steel frame with a 2.5m × 2.5m floor plan and a height of 3.6m (Figure 5a). The columns were B100×9 sections and the floor beams were S75×11 sections, all sections were Grade 300 steel. The beams and columns were bolted together. Bracing was added in all bays with two 12.7mm diameter threaded steel rods, see Figure 5b. Additional mass was distributed around the structure to make it more realistic. Four 1000kg floor slabs were placed on the 1st, 2nd and 3rd floors, one per bay. On the 4th floor, four 750kg slabs were used. Two of the slabs per floor were placed off-centre to increase the coupling between translational and torsional motion.

In the following discussions the locations in the structure are referred to using their respective geographical directions of north (N), south (S), east (E) and west (W).

A total of 9 damage scenarios were simulated on the structure, these involved the removal of bracing and the loosening of bolts in the floor beam connections. Table 4 lists the damage states and gives a description of damage. The different configurations give a mixture of minor and extensive damage cases. In this study, damage configurations 1-7 were used.

A series of ambient and forced vibration tests were carried out on the structure. Of primary interest in this study were the forced random vibration tests conducted using an electro-dynamic shaker mounted on the SW bay of the 4th floor on the diagonal. Input into the shaker was band-limited 5-50Hz white noise. The structure was instrumented with 15 accelerometers; three accelerometers each for the base, 1st, 2nd, 3rd and 4th floors. These were located on the E and W frames to measure motion in the N-S direction and in the centre to measure E-W motion. Acceleration data was recorded at 200Hz using a

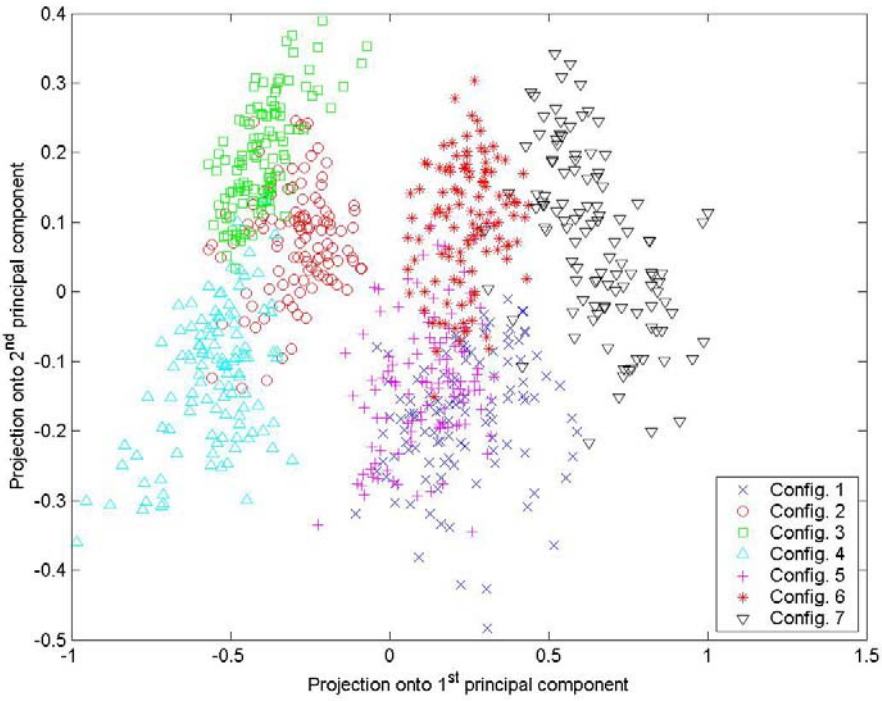

Figure 6. Projection of data from ASCE Phase II Experimental SHM Benchmark Structure onto the first two principal components.

data acquisition system and filtered with anti-aliasing filters.

Univariate AR(20) models were fitted to the acceleration data from each of the 15 accelerometers. This resulted in the dimension of feature (AR coefficient) vectors of 300. The AR coefficients were estimated using least squares from 1000-point segments advancing 200 points until the end of the record was reached. A data set of 805 feature vectors was obtained, 115 from each configuration.

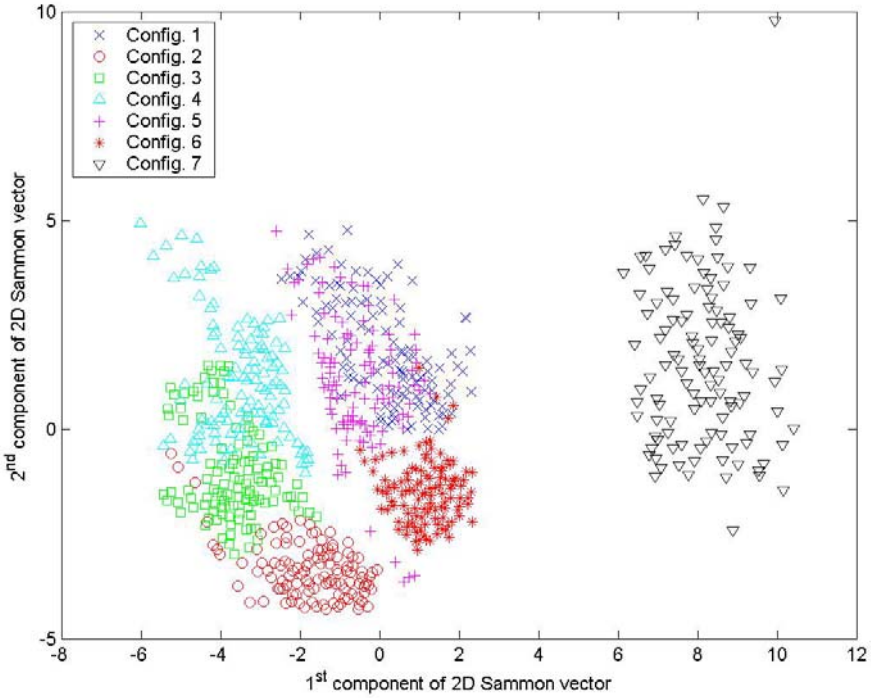

Figure 7. Projection of data from ASCE Phase II Experimental SHM Benchmark Structure via Sammon mapping.

Table 5. Number and percentage of misclassifications using NNC for ASCE Phase II Experimental SHM Benchmark Structure.

Number of principal components	Euclidean distance	Mahalanobis distance
20	0 (0%)	0 (0%)
10	2 (1%)	2 (1%)
5	9 (4.5%)	9 (4.5%)

Table 6. Number and percentages of misclassifications using LVQ for ASCE Phase II Experimental SHM Benchmark Structure.

Number of principal components	Number of codebook vectors		
	50	100	200
20	1 (0.5%)	1 (0.5%)	0 (0%)
10	6 (3%)	3 (1.5%)	2 (1%)
5	10 (5%)	12 (6%)	7 (3.5%)
3	26 (13%)	26 (13%)	27 (13.5%)

4.1 *Damage classification in the ASCE Phase II Experimental SHM Benchmark Structure*

Preliminary investigations showed that projection of the data onto the first two principal components allows much clearer clustering in the data to be seen than in the case of the 3-storey bookshelf structure (Figure 6). Three larger clusters are apparent that consist of the configurations 2-4, configurations 1, 5-6 and configuration 7, respectively. Some small to moderate degree of overlap generally exists between clusters corresponding to different damage configurations, but for configurations 1 and 5 the overlap is particularly strong. Using Sammon mapping, see Figure 7, a similar result was obtained, however configuration 7 appeared to be further isolated from the other configurations.

For the purpose of damage classification using NNC and LVQ, the feature dimension was reduced by projection of the data onto the first 20, 10, 5 or 3 principal components. The 805-point data set was randomly divided into 605 codebook vectors and 200 testing points. Using NNC and averaging the results from five runs with different selection of codebook vectors, the number of misclassifications and percentage errors are given in Table 5. In this case, similar performance was obtained using both the Euclidian and Mahalanobis distance measures. This can be attributed to the fact that the data from different damage configuration seems to be well separated. Very good performance (1% of misclassifications) was obtained using only 10 principal components. For 20 principal components, there were no misclassifications. These results represent significant reduction in dimensionally while good accuracy was maintained.

LVQ classification was applied to PCA-reduced data with the same number of principal components as previously and the same sized training and testing data sets were used. The results from NNC showed that performance was similar for both distance measures, and hence only the Euclidean distance was chosen for LVQ. The number of codebook vectors was either 50, 100 or 200. These were initialised by random selection from the training set. The results obtained from averaging the number of misclassifications from five runs are shown in Table 6. Overall, performance was similar to NNC but required significantly less codebook vectors. Excellent performance with less than 1% of misclassifications was obtained using 20 principal components for all numbers of codebook vectors. Errors became more significant (more than 5% of misclassifications) once fewer than five principal components were used.

5 **CONCLUSIONS**

SHM and damage detection methods can benefit from the applications of time series analysis techniques, which were developed for understanding long, regularly sampled sequences of data. In this study, a damage detection and classification method using AR models and NNC and LVQ statistical pattern recognition algorithms has been developed and applied to a simple 3-storey laboratory bookshelf structure and more complex ASCE Phase II Experimental SHM Benchmark Structure. Acceleration time histories of the structures in different simulated damage cases and under dynamic excitation were recorded and fitted using AR models. The coefficients of these AR models were chosen as damage sensitive features. Dimensionality reduction of the damage sensitive feature was achieved via PCA and Sammon's mapping and served the purpose of visualisation of clusters amongst the AR coefficients and lessening computational burden of the pattern recognition techniques. Systematic damage classification was studied using the NNC and LVQ supervised learning algorithms with either Euclidian or Mahalanobis distance measures, and different numbers of principal components and codebook vectors.

The studies on the 3-storey laboratory structure demonstrated that for localized stiffness reduction of 7% to 10% the AR coefficient corresponding to different damage states, when projected on two dimensions, do not form clearly separable clusters. However, when the number of principal components used was increased to 20 or more, both NNC and LVQ with Mahalanobis distance measure were able to classify damage with not more than approximately 1% of misclassifications. The Euclidian measure, on the other hand, produced nearly 20% of misclassifications. For the data from the ASCE Phase II Experimental SHM Benchmark Structure much more clearly delineated clusters of

AR coefficients can be seen in two dimensions. The results of a systematic damage classification using NNC and LVQ showed that classification accuracy similar to the 3-storey bookshelf structure can be achieved using 10 or more principal components. In this case the performance of both distance measures was comparable. Overall, the results showed that AR coefficients perform well as damage sensitive features, NNC and LVQ are reliable tools for damage classification, and significant reductions in the data dimensionality could be achieved whilst maintaining good performance.

ACKNOWLEDGEMENT

The authors would like to express their gratitude for the Earthquake Commission Research Foundation for their financial support of this research (Project No. UNI/535).

References:

ASCE Structural Health Monitoring Committee (2002). ASCE SHM benchmark webpage http://cive.seas.wustl.edu/wusceel/asce.shm/.

Doebling, S. W., Farrar, C. R., Prime, M. B., & Shevitz, D. W. (1996) Damage identification and health monitoring of structural and mechanical systems from changes in their vibration characteristics: A literature review, Los Alamos National Laboratory, Los Alamos, New Mexico.

Gul, M., Catbas, F. N., & Georgiopoulos, M. (2007). Application of pattern recognition techniques to identify structural change in a laboratory specimen. Sensors and Smart Structures Technologies for Civil, Mechanical and Aerospace Systems 2007, San Diego, 65291N1-65291N10.

Kohonen, T. (1997). Self-organizing Maps, Springer, Berlin.

Nair, K. K., Kiremidjian, A. S., & Law, K. H. (2006). Time series-based damage detection and localization algorithm with application to the ASCE benchmark structure. Journal of Sound and Vibration, 291(1-2), 349-368.

Nair, K. K., & Kiremidjian A. S. (2007). Time series based structural damage detection algorithm using Gaussian Mixtures Modeling. Journal of Dynamic Systems, Measurement and Control, Transactions of the ASME, 129(3), 285-293.

Omenzetter, P., & Brownjohn, J. M. W. (2006). Application of time series analysis for bridge monitoring. Smart Materials and Structures, 15(1), 129-138.

Sammon, J. J. W. (1969). Nonlinear mapping for data structure analysis. IEEE Transactions on Computers, C-18(5), 401-409.

Sharma, S. (1997). Applied Multivariate Techniques, Wiley, New York.

Sohn, H., Czarnecki, J. A., & Farrar, C. R. (2000). Structural Health Monitoring using statistical process control. Journal of Structural Engineering, 126(11), 1356-1363.

Sohn, H., Farrar, C. R., Hunter, N. F., & Worden, K. (2001). Applying the LANL statistical pattern recognition paradigm for structural health monitoring to data from a surface-effect fast patrol boat. Los Alamos National Laboratory, Los Alamos, New Mexico.

Sohn, H., Farrar, C. R., Hemez, F. M., Shunk, D. D., Stinemates, D. W., & Nadler, B. R. (2003) A review of Structural Health Monitoring literature: 1996–2001. Los Alamos National Laboratory, Los Alamos, New Mexico.

Wei, W. W. S. (2006). Time Series Analysis: Univariate and Multivariate Methods, Pearson, Boston.